Effect of the charge-carrier–phonon interaction on the fundamental $1/f$ voltage noise

Kirill A. Kazakov [*]

Department of Theoretical Physics, Physics Faculty, Moscow State University, 119991 Moscow, Russian Federation

It is known that quantum indeterminacy sets a lower bound on the power spectrum of voltage fluctuations in any conducting medium. The low-frequency asymptotic of this bound is $\sim 1/f$ in the case of freely propagating charge carriers. It is found that on account of the charge-carrier–phonon interaction, the asymptotic becomes $\sim 1/f^\gamma$, $\gamma \neq 1$. Its general expression is derived in the case of charge carriers subject to the piezoelectric interaction with acoustic phonons. The sign of $(\gamma - 1)$ depends on the state filling for charge carriers, so that γ may exceed unity despite the absence of a low-frequency cutoff. It is shown that under stationary physical conditions the voltage variance grows with time as $t^{\gamma-1}$, in agreement with observations. It is proved that despite this growth the power spectrum is well defined and finite for $\gamma < 2$. A practical attainability of the quantum bound is discussed. A comparison with the experimental data on $1/f$ noise in InGaAs quantum wells and high-temperature superconductors is made. It is demonstrated that the account of $\gamma \neq 1$ brings the calculated noise levels uniformly within an order of magnitude of the measured. This holds true whether the voltage fluctuations are measured along or across the electric current, though the observed noise levels in the two cases are significantly different.

I. INTRODUCTION

It is experimentally established that power spectra of the voltage fluctuations in all conducting media exhibit a universal low-frequency behavior: for sufficiently small frequencies f, the power spectral density $S(f) \sim 1/f^\gamma$, where the frequency exponent γ is around unity [1–4]. These ubiquitous fluctuations are often called simply $1/f$, or flicker, noise. It has been detected at frequencies as high as 10^6 Hz down to $10^{-6.3}$ Hz [5,6], with no sign of low-frequency spectrum flattening.

There are various physical processes producing voltage noise: the charge carrier trapping-detrapping, motion of dislocations, conductance fluctuations caused by the temperature fluctuations, etc. The so-called $1/f$ problem can be broadly formulated as a difficulty to relate $1/f$ spectrum to any of these conventional noise sources. In fact, it is hard to indicate a physical process, say, in a crystal of pure copper, which would be characterized by frequencies much lower than 1 Hz. Furthermore, in specific experiments, $1/f$ noise is often observed over frequency bands five to six decades wide (see, e.g., Refs. [5–10], to mention a few), whereas the bandwidths of noise produced by the above-mentioned mechanisms are significantly more narrow. For example, defect motion in carbon conductors gives rise to the $1/f$ spectrum only in the range $f \approx 10^2$–10^4 Hz [11]. By the same reason, theories based on the charge-carrier trapping-detrapping mechanism [12,13] have been generally unsuccessful either. Namely, if the $1/f$ noise observed in a given frequency range is supposed to originate from the charge-carrier trapping, the inverse trapping times need to be finely distributed over a much wider range in such a way that the Lorentzians produced by individual traps would sum up to the observed spectrum [14]. Not saying that this mechanism fails in metals, and leaving aside its quantitative part (which demands not only the frequency profile, but also the noise magnitude be accounted for), to explain the formation of such a perfect distribution is itself a difficult task. In practice, on the other hand, contributions of the conventional noise sources are usually easily identified based on the known material properties and the sample preparation techniques.

The *fundamental* $1/f$ *noise* is what remains after all conventional contributions have been eliminated, either analytically in the course of spectrum postprocessing by using appropriate models for the noise mechanisms involved, or experimentally, by improving the sample preparation technology. According to the quantum theory of fundamental $1/f$ noise [15–17], it is generated by quantum fluctuations of the electromagnetic field produced by freelike charge carriers, rather than by fluctuations in the material properties of the conducting medium. Somewhat more specifically, fluctuations of the electric voltage measured between two probes attached to the sample are correlated via their interaction with the same (partially) filled charge-carrier state. By this reason, the process can be termed one-particle, though the net effect is an average over many individual contributions. Thus, the properties of the medium in this picture are important only to the extent that they affect the charge-carrier propagation.

In Refs. [15,16], flicker noise is considered as an essentially thermal effect related to the photon heat bath, so that its contribution to the voltage power spectrum vanishes in the state of photon vacuum. However, it was shown recently that the quantum $1/f$ noise actually does not vanish at zero temperature, remaining at a finite level determined by quantum uncertainty in the values of voltage measured at

_____

[*]kirill@phys.msu.ru

different times [17]. The consideration of Ref. [17] was restricted by the assumption that the charge carriers are freelike; namely, their collisions have a negligible effect on the noise power spectrum. The latter was found to be inversely proportional to frequency, that is, the frequency exponent exactly equal to unity, $\gamma = 1$. On the other hand, the experimentally measured γ's are never strictly equal to unity, if only because of the inevitable experimental errors. This fact raises two important questions. First, what is the measure of smallness of $(\gamma - 1)$ which would help one decide whether it is really negligible? The point is that γ is the exponent of a dimensional quantity, so that its deviation from unity brings in a new dimensional parameter into the power spectrum. In fact, a pure $1/f$ noise power spectrum is generally of the form $S(f) = \varkappa U_0^2/|f|$, where U_0 is the voltage bias applied to a sample, and $\varkappa$ is a dimensionless constant dependent on the sample properties. As γ deviates from unity, this constant becomes dimensional, $\varkappa \to \varkappa(f_*)^\delta$, where $\delta \equiv \gamma - 1$ and f_* is a constant with the dimension of frequency. The possibility to replace $1/f^\gamma$ by $1/f$ is thus directly related to the value of this parameter. But f_* is naturally expected to be very large when measured in hertz, because it is on the order of the inverse characteristic time of whatever microscopic process is responsible for the frequency exponent deviation. We see that there is a strong correlation between $(\gamma - 1)$ and the noise magnitude. Unfortunately, this circumstance is often ignored, and determination of γ is not paid due attention in experimental studies. Authors usually content themselves by a mere check that γ is close to unity, to neglect its deviation therefrom altogether. This is probably because to accurately determine γ requires sufficiently large frequency spans, usually three to four decades to achieve an experimental error less than 0.05. Undoubtedly, this sensitivity of the noise magnitude to the value of δ is one of the main reasons why the numerous empirical attempts to come closer to the flicker noise origin have been inconclusive.

The second important question related to the frequency exponent deviation is that in the absence of a low-frequency cutoff, allowing for $\gamma > 1$ leads to an apparent conflict with the observed finiteness of the voltage variance. In fact, a direct consequence of the Wiener-Khinchin relation [18,19] is that this variance is equal to $2 \int_0^\infty df\, S(f) = \infty$. The divergence of this integral at $f = 0$ is immaterial for $\gamma = 1$ (in which case the divergence is only logarithmic), in view of the existence of a natural low-frequency cutoff, f_0—the inverse lifetime of the universe, which bounds the total noise power to reasonably moderate values [20]. But this argument does not resolve the problem for $\gamma > 1$, because $\int df\, S(f) \sim 1/f^{\gamma-1}$ would be unacceptably large for many actual spectra continued down to f_0. The purpose of the present paper is to answer these questions. It will be shown that account of the charge-carrier interaction with acoustic phonons modifies the frequency exponent in such a way that $(\gamma - 1)$ can be positive as well as negative. In particular, the corresponding dimensional parameter in the power spectrum will be identified (previously, deviations of γ from unity were taken into account only formally using the techniques of dimensional continuation [16]). This will be done in the simplest case of a parabolic energy-momentum dispersion for the charge carriers. Also, it will be demonstrated explicitly how the quantum

indeterminacy resolves an apparent conflict of $\gamma > 1$ with the Wiener-Khinchin theorem in the absence of a low-frequency cutoff.

The paper is organized as follows. Basic results of the new approach to the $1/f$ problem are summarized in Sec. II A. Section II B describes the physical model and the method of calculating the voltage power spectrum. The way the charge-carrier–phonon interaction shows itself in the present context is discussed in detail in Sec. III B. The low-frequency asymptotic of the power spectrum is then evaluated in Sec. III. Its explicit expressions are obtained for two measurement setups—the basic longitudinal and a less common transverse configuration. After a general analysis of practical attainability of the quantum bound, comparisons with the experimental data in semiconductors and high-temperature superconductors are made in Sec. IV. The obtained results are further discussed in Sec. V where conclusions are drawn. The paper has an Appendix where some general issues of the quantum approach to the $1/f$ problem are taken up.

II. THE NOISE POWER SPECTRAL DENSITY

A. Quantum bound on the voltage power spectrum

For the sake of completeness, we begin by summarizing basic results of the quantum approach to the fundamental $1/f$ noise [17].

Consider a (semi)conducting sample with a constant electric current through it supplied by two leads attached to the sample. For simplicity, the sample material will be assumed macroscopically homogeneous, and so will be the electric field, $\boldsymbol{E}$, established inside. Let the voltage across the sample be measured by means of two voltage probes which may or may not coincide with the current leads. Also for simplicity, the probes will be considered pointlike, $\boldsymbol{x}_1, \boldsymbol{x}_2$ denoting their position. From the quantum theory standpoint, the voltage $U(t, \boldsymbol{x}_1, \boldsymbol{x}_2)$ measured between the probes at time t is an observable to which there corresponds a Hermitian (Heisenberg) operator $\widehat{U}(t)$ (for brevity, the arguments $\boldsymbol{x}_1, \boldsymbol{x}_2$ are henceforth suppressed). For a given constant bias U_0, this defines another observable: the voltage fluctuation

$$\widehat{\Delta U}(t) = \widehat{U}(t) - U_0. \tag{1}$$

The power spectrum of a signal measured during time t_m is given, as usual, by

$$S(f) = \lim_{t_m \to \infty} \frac{1}{t_m}\{\langle(\widehat{\Delta U_s}(\omega))^2\rangle + \langle(\widehat{\Delta U_c}(\omega))^2\rangle\}, \quad \omega = 2\pi f, \tag{2}$$

where

$$\widehat{\Delta U_s}(\omega) = \int_0^{t_m} dt\, \widehat{\Delta U}(t)\sin(\omega t),$$

$$\widehat{\Delta U_c}(\omega) = \int_0^{t_m} dt\, \widehat{\Delta U}(t)\cos(\omega t), \tag{3}$$

and $\langle \hat{f} \rangle = \mathrm{tr}(\hat{\rho}\hat{f})$, $\hat{\rho}$ being the system density matrix. A crucial point is that the power spectrum as defined by Eq. (2) is free of the operator-ordering ambiguity suffered by the voltage autocorrelation function.

The minimum value, $S_F(f)$, of the power spectrum is determined by the commutator of $\widehat{\Delta U_s}(\omega)$, $\widehat{\Delta U_c}(\omega)$,

$$S_F(f) = \lim_{t_m \to \infty} \frac{1}{t_m} |\langle [\widehat{\Delta U_s}(\omega), \widehat{\Delta U_c}(\omega)] \rangle|, \qquad (4)$$

and is identified as the power spectrum of fundamental noise. It is important that the expectation value on the right-hand side of Eq. (4) is an odd function of frequency, so that S_F is determined by the Fourier transform of a contribution to $\langle \widehat{\Delta U}(t) \widehat{\Delta U}(t') \rangle$ which is antisymmetric under the interchange $t \leftrightarrow t'$,

$$\langle [\widehat{\Delta U_s}(\omega), \widehat{\Delta U_c}(\omega)] \rangle = \iint_0^{t_m} dt\, dt'\, \langle [\widehat{\Delta U}(t), \widehat{\Delta U}(t')] \rangle$$
$$\times\, \sin(\omega t) \cos(\omega t')$$
$$= \iint_0^{t_m} dt\, dt'\, \langle \widehat{\Delta U}(t) \widehat{\Delta U}(t') \rangle$$
$$\times\, \sin(\omega(t - t')). \qquad (5)$$

This fact allows the use of the standard momentum-space techniques of quantum field theory to extract the low-frequency asymptotic of $S_F(f)$.

Because of the factor $1/t_m$ in Eq. (4), the only terms that contribute in the limit $t_m \to \infty$ are those dependent solely on $(t - t')$. Designating them by a minus subscript, $\langle \widehat{\Delta U}(t) \widehat{\Delta U}(t') \rangle_- \equiv S(t - t')$, it is convenient to introduce an auxiliary function

$$\Sigma(f) = \lim_{t_m \to \infty} \frac{1}{t_m} \iint_0^{t_m} dt\, dt'\, S(t - t') e^{i\omega(t - t')}.$$

On applying Euler's formula to the integrand, the contribution of cosine to $\Sigma(f)$ is just $S(f)$, whereas the modulus of the other contribution is $S_F(f)$. A straightforward calculation brings $\Sigma(f)$ to the form

$$\Sigma(f) = \lim_{t_m \to \infty} \left\{ \int_{-t_m}^{t_m} d\tau\, S(\tau) e^{i\omega\tau} - \frac{1}{t_m} \int_{-t_m}^{t_m} d\tau\, |\tau| S(\tau) e^{i\omega\tau} \right\}. \qquad (6)$$

If $S(\tau)$ is assumed to sufficiently rapidly decrease as $|\tau| \to \infty$, the second term in braces vanishes in the limit $t_m \to \infty$, and Eq. (6) takes on the appearance of a Wiener-Khinchin relation. But $1/f$ noise is just the case where this assumption is invalid. Namely, it will be shown below that on account of the charge-carrier–phonon interaction, $S(\tau) \sim |\tau|^{\gamma - 1}$, and the presence of this term guarantees that the limit of the braced expression exists.

B. Physical model and the method of calculating $S_F(f)$

We consider the charge carriers in the sample as nonrelativistic fermions with the electric charge e and effective mass m, which is sufficient for most practical applications. For simplicity, they will be taken unpolarized, and all spin indices will be suppressed throughout. According to Ref. [17], a system comprised of freelike charge carriers and photons generates voltage fluctuations which are characterized by a pure $1/f$ power spectrum, $S(f) = \varkappa U_0^2 / |f|$. This conclusion is universal in that it holds for any charge-carrier energy-momentum dispersion; it is the reduced power spectrum, $\varkappa$,

that only depends on the charge-carrier specifics, in particular on its effective mass. The space dimensionality does not affect the frequency exponent either until the dielectric response of the medium is taken into account. Though these statements follow from a lengthy explicit calculation [17], they can be easily understood on dimensional grounds. The point is that at zero temperature one cannot build a dimensionless quantity out of the parameters characterizing the charge-carrier dispersion which could appear in the frequency exponent. In fact, the only such dimensionless quantity—the fine structure constant $\alpha = e^2 / \hbar c \approx 1/137$—is independent of the charge-carrier properties. It will appear in the frequency exponent once the relativistic radiative corrections to the charge-carrier propagator due to the vacuum polarization are taken into account. On account of these corrections, the pole of the momentum-space electron propagator, $D(p)$, is modified according to

$$D(p) \sim (p^2 - m^2)^{-1} \rightarrow (p^2 - m^2)^{-1} \left(\frac{m^2}{|p^2 - m^2|} \right)^{\alpha/\pi},$$

where m is the free electron mass, and p is its 4-momentum (see, e.g., Ref. [21]). The exponent α/π eventually converts into the frequency exponent of the voltage power spectrum, but this contribution is tiny according to the smallness of relativistic vacuum polarization effects at the charge-carrier energies characteristic for ordinary solids. Yet, this observation suggests that a similar nonrelativistic effect related to the vacua of other quasiparticles present in the system might give rise to a noticeable deviation of the frequency exponent. Thus, we include phonons into the list of the system constituents to take into account the charge-carrier interaction with the lattice vibrations. This interaction is normally a primary factor that affects the charge-carrier propagation, whereas the phonon radiation effects bear a great deal of similarity to those involving photons. Its detailed description will be given later on in this section. Regarding thermal effects, we discard those related to the photon heat bath for the reason already mentioned in the Introduction. As to the phonon heat bath, calculations show that it is virtual phonon contributions which give rise to the frequency exponent deviation. Therefore, to simplify the presentation, real phonons will be excluded from consideration from the outset. On the other hand, dependence of the charge-carrier density matrix on temperature is of practical importance, and so in the general formulation given below it is kept arbitrary.

As was mentioned above, the power spectrum of fundamental noise is determined by an odd in $\tau = t - t'$ part of the function $\langle \widehat{\Delta U}(t) \widehat{\Delta U}(t') \rangle_-$. Using the Schwinger-Keldysh technique [22,23], this expectation value can be written as

$$\langle \widehat{\Delta U}(t) \widehat{\Delta U}(t') \rangle$$
$$= \text{tr} \left(\hat{\rho}_0 \mathcal{T}_C \widehat{\Delta u}^{(2)}(t) \widehat{\Delta u}^{(1)}(t') \exp \left\{ -i \int_C dt\, \hat{w}(t) \right\} \right), \quad (7)$$

where $\hat{w}(t)$ is the interaction Hamiltonian, $\hat{\rho}_0$ is the density matrix of noninteracting particles—charge carriers, photons, and phonons (lowercase letters denote operators in the interaction picture), and the so-called Schwinger-Keldysh time contour C runs from $t = -\infty$ to $t = +\infty$, and then back to $t = -\infty$, for which the forward branch is designated with

a superscript (1) and treated as being in the past with respect to any instant on the backward branch designated with a superscript (2). $\mathcal{T}_C$ accordingly orders all operators along the contour C: it is chronological on the forward branch of C, and antichronological on its backward branch. In Eq. (7), $\widehat{\Delta u}(t)$ and $\widehat{\Delta u}(t')$ are assigned the superscripts (2) and (1), respectively, because their product on the left-hand side is not time ordered, $\widehat{\Delta U}(t)$ standing to the left of $\widehat{\Delta U}(t')$ for all t, t'. To simplify intermediate expressions, we use units in which $\hbar = c = 1$, c denoting the speed of light in vacuum.

The right-hand side of Eq. (7) is suitable for a perturbative expansion with respect to whatever couplings appear in $\hat{w}(t)$. Since we presently neglect thermal effects related to the heat bath of photons and phonons, the system density matrix $\hat{\rho}_0$ reduces to that of the charge carriers, $\hat{\varrho}$, times the photon and phonon vacua. As usual, on expanding the right-hand side of Eq. (7) in powers of the coupling constants and using the macroscopic Wick theorem, it is expressed as the sum of products of particle propagators. There are four propagators for each particle, depending on which branch of the contour C the time arguments of the propagator belong to. Thus, the fermion propagator is a matrix

$$D^{(ij)}(x, y) = \text{tr}(\hat{\varrho}\mathcal{T}_C\hat{\phi}^{(i)}(x^0, \boldsymbol{x})\hat{\phi}^{(j)\dagger}(y^0, \boldsymbol{y})), \quad (8)$$

where $\hat{\phi}$ is the fermion field, indices i, j take on values 1,2, and the action of $\mathcal{T}_C$ is extended over single-field operators by specifying that an interchange of two fermionic operators is accompanied by a factor of (-1). Using the standard momentum-space decomposition of $\hat{\phi}(x^0, \boldsymbol{x})$, the charge-carrier propagator can be written as the sum

$$D^{(ij)}(x, y) = D_0^{(ij)}(x, y) + \Delta(x, y)$$

of a vacuum part

$$D_0^{(ij)}(x, y) = \int_{-\infty}^{+\infty} \frac{d^4 p}{(2\pi)^4} D_0^{(ij)}(p)e^{-ip(x-y)},$$

$$D_0^{(11)}(p) = \frac{i}{p^0 - \varepsilon_{\boldsymbol{p}} + i0} = \left[D_0^{(22)}(p)\right]^*,$$

$$D_0^{(12)}(p) = 0, \quad D_0^{(21)}(p) = 2\pi\delta(p^0 - \varepsilon_{\boldsymbol{p}}), \quad (9)$$

and of a part dependent on the charge-carrier state,

$$\Delta(x, y) = \int_{-\infty}^{+\infty} \frac{d^3\boldsymbol{q}}{(2\pi)^3}\frac{d^3\boldsymbol{q}'}{(2\pi)^3}\varrho(\boldsymbol{q}, \boldsymbol{q}')e^{-i(\varepsilon_q x^0 - \varepsilon_{q'}y^0)+i(\boldsymbol{q}\cdot\boldsymbol{x}-\boldsymbol{q}'\cdot\boldsymbol{y})}, \quad (10)$$

where $\varrho(\boldsymbol{q}, \boldsymbol{q}')$ is the momentum-space density matrix of charge carriers. It is to be noted that this matrix is not diagonal, because charge carriers are bound to pass through a sample of finite dimensions.

Likewise, the photon propagator matrix reads, in the Feynman gauge,

$$G_{\mu\nu}^{(ij)}(x, y) = -4\pi\eta_{\mu\nu}\int_{-\infty}^{+\infty} \frac{d^4 k}{(2\pi)^4}G^{(ij)}(k)e^{-ik(x-y)},$$

$$G^{(11)}(k) = \frac{i}{k^2 + i0} = [G^{(22)}(k)]^*,$$

$$G^{(12)}(k) = 2\pi\theta(-k^0)\delta(k^2),$$

$$G^{(21)}(k) = 2\pi\theta(k^0)\delta(k^2), \quad (11)$$

where $\theta(k^0)$ is the step function [$\theta(k^0) = 0$ for $k^0 \leqslant 0$, $\theta(k^0) = 1$ for $k^0 > 0$]. From here on, the space-time or momentum-energy coordinates and integrals are written as "four dimensional," $x = (x^0, \boldsymbol{x})$, $k = (k^0, \boldsymbol{k})$, $kx = k^0 x^0 - \boldsymbol{k}\cdot\boldsymbol{x}$.

Similarly to photons, the phonon propagator is a 2×2 matrix $C^{(ij)}$ of which only its (11) component will be needed below explicitly. It reads, in momentum space,

$$C^{(11)}(l) = \frac{2i\omega_l}{(l^0)^2 - \omega_l^2 + i0},$$

where $\omega_l = u|\boldsymbol{l}|$, u denoting the acoustic wave velocity.

The products of particle propagators are integrated over time with appropriate vertex factors generated by the interaction Hamiltonian $\hat{w}(t)$, each vertex belonging to either branch of the contour C. It is convenient to let all time integration variables run from $-\infty$ to $+\infty$; vertices on the backward branch will then carry an extra factor of (-1). Otherwise, the rules of calculating expression (7) are the same as for two-point Green's functions in the scattering theory.

The Hamiltonian of electromagnetic interaction of nonrelativistic charge carriers reads

$$\hat{w}(t) = \int d^3\boldsymbol{x}\hat{\phi}^\dagger(x)\left[e\hat{a}_0(x) + \frac{e^2}{2m}\boldsymbol{a}^2(t) + \frac{ie}{m}\boldsymbol{a}(t)\cdot\boldsymbol{\nabla}\right]\hat{\phi}(x), \quad (12)$$

where $\boldsymbol{a}(t)$ is the vector potential of homogeneous external electric field,

$$\boldsymbol{a}(t) = i\boldsymbol{E}\frac{e^{i\lambda t} - 1}{\lambda}, \quad \lambda \to 0. \quad (13)$$

According to the gauge choice, a direct Coulomb interaction of charge carriers is excluded from the interaction Hamiltonian [24,25]. In momentum space, the Hamiltonian (12) generates three types of vertex factors: a factor e of the charge-carrier interaction with the scalar electromagnetic potential a_0, and two factors of its interaction with the classical vector potential, $-e\boldsymbol{a}\cdot\boldsymbol{q}/m$ and $e^2\boldsymbol{a}^2/2m$.

It remains to specify the charge-carrier interaction with phonons. Regarding electric fluctuations produced by the charge carrier, of special importance is its long-range piezoelectric interaction with acoustic phonons. This is because this interaction modifies the pole structure of the charge-carrier propagator which is essential in determining the quantum bound. The piezoelectric effect is exhibited by many solids lacking inversion symmetry. Moreover, even if inversion is a bulk symmetry of the given pristine material, it is often broken by the presence of impurities, straining, or by finite-size effects. As a result, the material may become a strong piezoelectric, as is the case, for instance, with graphene [26,27]. The Hamiltonian of piezoelectric interaction of the charge carriers with acoustic phonons is, in momentum representation,

$$\hat{w}_{\text{ep}} = i\sum_l \frac{M_\lambda(\tilde{\boldsymbol{l}})}{\sqrt{2\omega_l\rho_0\Omega_0}}\hat{n}(\boldsymbol{l})(\hat{a}_l + \hat{a}_{-l}^\dagger), \quad (14)$$

where $\hat{a}_l$ are the phonon destruction operators, $\hat{n}(\boldsymbol{l})$ is the Fourier transform of the charge-carrier density, ρ_0 is the
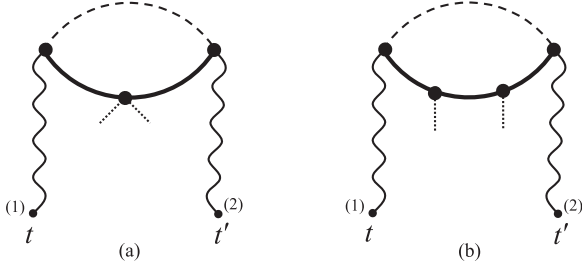
FIG. 1. Feynman diagrams representing contributions to $S(\tau)$ of the lowest order with respect to the electromagnetic coupling. Thick symbols depict dressing by the charge-carrier–phonon interaction. Solid lines denote $\mathcal{D}_0$, dashed lines Δ, and wavy lines photon propagators; each dotted line designates a factor of $\boldsymbol{E}$.

sample density, Ω_0 is the quantization volume, and $M_\lambda(\tilde{\boldsymbol{l}}) = -M_\lambda^*(-\tilde{\boldsymbol{l}})$ is the piezoelectric matrix element which depends only on the phonon wave-vector direction $\tilde{\boldsymbol{l}} = \boldsymbol{l}/|\boldsymbol{l}|$. A detailed derivation of this Hamiltonian and discussion of the underlying physics can be found in Ref. [28]. The meaning of summation over phonon momenta in the present context is the following. Consider an acoustic wave propagation in a system comprised of the sample, say, a thin film, a substrate it is grown on, and a current source including the wires connecting it to the sample via the current leads. This propagation essentially depends on the acoustic impedance ratios of the system elements. In an idealized case of no reflection at the current leads, acoustic waves propagate as if the system was of infinite extent. In other words, when counting the phonon states and performing summations thereon, the quantization volume Ω_0 can be considered as large as needed to justify these operations and to replace the sum over $\boldsymbol{l}$ by an integral.

As the elements of Feynman diagrams, D_0 and Δ will be depicted by solid and dashed lines, respectively, photon propagators by wavy lines, and phonon propagators by dash-dotted lines. Each factor of $\boldsymbol{E}$ will be symbolized by a dotted line. In momentum space, D_0 and $G_{\mu\nu}$ are functions of the corresponding particle 4-momenta, in contrast to Δ which depends on a pair of 3-momenta $\boldsymbol{q}, \boldsymbol{q}'$, or in the four-dimensional notation, on the charge-carrier 4-momenta on the mass shell, $q = (\varepsilon_{\boldsymbol{q}}, \boldsymbol{q})$ and $q' = (\varepsilon_{\boldsymbol{q}'}, \boldsymbol{q}')$.

III. EVALUATION OF THE LOW-FREQUENCY ASYMPTOTIC OF $S_F(f)$

A. Extraction of the leading term of $\langle \widehat{\Delta U}(t) \widehat{\Delta U}(t') \rangle_-$

As in the case of pure $1/f$ noise, the lowest-order contribution to S_F with respect to the external electric field is represented by two basic diagrams in Fig. 1. The difference is that the charge-carrier propagators and vertices of their electromagnetic interaction are now modified by the charge-carrier–phonon interaction, which is depicted by thickening their graphic symbols. Diagrams of the type in Fig. 1(b) turn out to cancel each other, so it is diagrams in Fig. 1(a) which only contribute to S_F. According to the Schwinger-Keldysh rules, each interaction vertex is assigned an index that takes on values 1 and 2. Thus, there are eight different diagrams of the same basic structure as in Fig. 1(a), but only four of
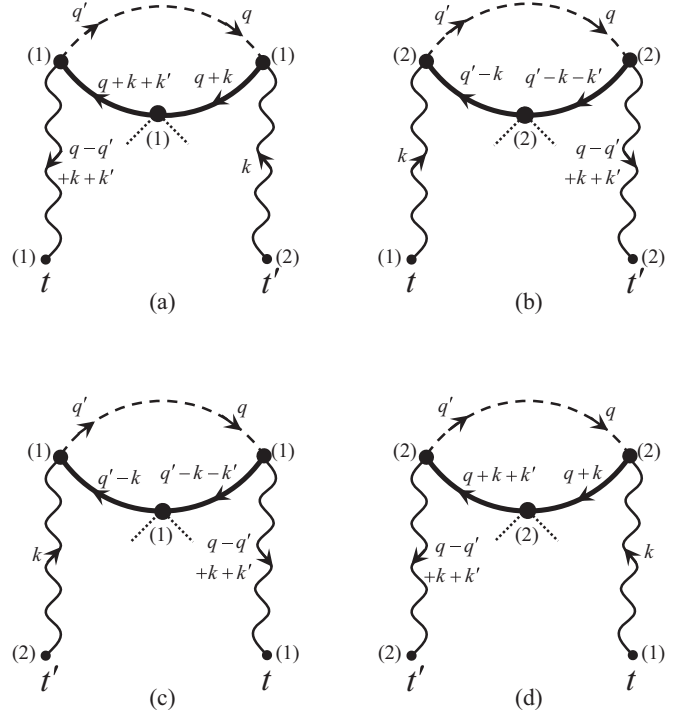

FIG. 2. Nonvanishing diagrams representing the basic diagram in Fig. 1(a) in the Schwinger-Keldysh formalism. Arrows on the lines show the energy-momentum flow.

them are nonvanishing. This is because a free charge carrier cannot emit a real photon (by virtue of the energy-momentum conservation), and so all interaction vertices in Fig. 1 must be of the same type—either (1) or (2) [notice also that $D_0^{(12)}(p) \equiv 0$]. This leaves us with four diagrams of the basic type in Fig. 1(a) which are drawn in Fig. 2. Arrows on the lines show the momentum flow; those on the charge-carrier propagators are concurrent with the direction from $\hat{\phi}^\dagger$ to $\hat{\phi}$. A line with the 4-momentum k coming in into a vertex with the 4-coordinates x brings in a factor of e^{-ikx}. In particular, k in all cases is assigned to the photon propagators $G^{(12)}$ and $G^{(21)}$, so that it satisfies $k^2 = 0$ [cf. Eq. (11)]. The 4-momentum associated with the vector potential (13) is $(\lambda, \boldsymbol{0})$. Therefore, the momentum coming in into the interaction vertex $\sim \boldsymbol{a}^2$ is $k' = (\lambda + \lambda', \boldsymbol{0})$, with each of λ, λ' being related to one of the factors $\boldsymbol{a}$ by Eq. (13).

Each diagram in Fig. 2 involves a factor of Δ (dashed line), which is proportional to $\varrho(\boldsymbol{q}, \boldsymbol{q}')$. The latter represents the one-particle density matrix of charge carriers, and is normalized according to $\mathrm{tr}\hat{\varrho} = N$, where $N \gg 1$ is the number of charge carriers in the sample. This does not mean, however, that the power spectrum is proportional to N, because not every contribution to the integral over $\boldsymbol{q}, \boldsymbol{q}'$ in these diagrams also contributes to the power spectrum. It was mentioned in Sec. II A that the contributions surviving in the limit $t_m \to \infty$ are those which depend on t, t' via the difference $(t - t')$ only. Therefore, the time component of $(q - q' + k + k')$ must be equal to that of k [cf. 4-momenta assigned to the wavy lines in Fig. 2 and expression (11) for the photon propagator]. Since $k'^0 = \lambda + \lambda'$ is ultimately set equal to zero, the condition is $q^0 = q'^0$. Now, the charge-carrier energy in the sample

is quantized. Of course, the spacing of energy levels in a macroscopic sample is negligible in many respects, so that the spectrum can be considered quasicontinuous. But its actual discreteness turns out to be essential in the present context, because the above condition requires that the energies q^0 and q'^0 be the same energy eigenvalue. Therefore, in order to identify the nonvanishing terms in the power spectrum, one has to count the number of contributions satisfying this condition. We recall that the charge-carrier momentum is smeared in each energy eigenstate, and that the set of all momentum eigenstates is complete (as is the set of all energy eigenstates). That is, when the two integration variables q, q' run independently over all momenta, the corresponding energies run over all energy eigenvalues. Hence, for N occupied states, there is a total of N^2 pairs of states, of which only N have the same energy. Thus, the fraction of contributions to the power spectrum that satisfy the above condition is $1/N$. In effect, therefore, the density matrix associated with the dashed line in Fig. 2 is to be normalized by $\mathrm{tr}\hat{\varrho} = 1$ or, more explicitly,

$$\int \frac{d^3\boldsymbol{q}}{(2\pi)^3} \varrho(\boldsymbol{q}, \boldsymbol{q}) = 1. \tag{15}$$

We note also that it is this instance where the nondiagonality of the density matrix shows itself. $\varrho(\boldsymbol{q}, \boldsymbol{q}')$ is not diagonal because of finiteness of the sample volume, Ω. This fact is conveniently made manifest by expressing ϱ via the mixed position-momentum distribution function, $R(\boldsymbol{r}, \boldsymbol{Q})$, which vanishes for $\boldsymbol{r}$ outside of the sample,

$$\varrho\left(\boldsymbol{Q} - \frac{\boldsymbol{p}}{2}, \boldsymbol{Q} + \frac{\boldsymbol{p}}{2}\right) = \frac{1}{\Omega} \int_\Omega d^3\boldsymbol{r} e^{i\boldsymbol{p}\cdot\boldsymbol{r}} R(\boldsymbol{r}, \boldsymbol{Q}). \tag{16}$$

Probability distributions for the particle position in the sample or its momentum can be found by integrating $R(\boldsymbol{r}, \boldsymbol{Q})/\Omega$ over all momenta or the sample volume, respectively. At the same time, the dressed charge-carrier propagators (thick lines in Fig. 2) also involve the function Δ as part of the corrections due to the charge-carrier–phonon interaction. But since these propagators are diagonal in the charge-carrier momentum, they depend on the diagonal elements of $\varrho(\boldsymbol{q}, \boldsymbol{q}')$ only. ϱ entering these contributions is still normalized by $\mathrm{tr}\hat{\varrho} = N$, so that $\varrho(\boldsymbol{q}, \boldsymbol{q})$ is the *mean occupation number* $\nu(\boldsymbol{q})$, rather than the probability of state with the given $\boldsymbol{q}$.

As will be seen below, the principal effect of the charge-carrier–phonon interaction is to shift the frequency exponent, while its contribution to the prefactor is relatively small. Summarizing the above, it then follows that in the considered approximation, the *reduced power spectrum is independent of the number of charge carriers*.

It is important for the above consideration that the power spectrum is defined in the limit $t_m \to \infty$. In actual experiments, however, one always deals with finite measurement times which are usually $\sim 1/\omega$. To justify applicability of the obtained results in such circumstances, we note that for t_m on the order of $1/\omega$, the above energy condition is replaced by $|q^0 - q'^0| \lesssim \hbar\omega$. Therefore, the counting of relevant states remains the same until $\hbar\omega$ exceeds the energy spacing. The latter is $1/(D\Omega)$, where D is the density of states of charge carriers in the given material. We see that taking $t_m \sim 1/\omega$ is inconsequential with regard to the noise magnitude at
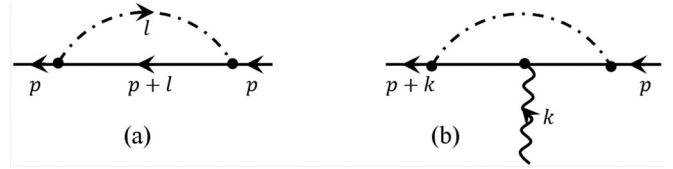

FIG. 3. Account of the charge-carrier interaction with phonons. (a) The lowest-order charge-carrier self-energy. (b) The lowest-order vertex correction.

sufficiently low frequencies,

$$\omega \lesssim \frac{1}{\hbar D\Omega}. \tag{17}$$

The density of states varies significantly from one solid to another, but virtually always $D \lesssim 10^{22}/(\mathrm{eV\,cm}^3)$, while the volume of samples used in the flicker noise studies is typically 10^{-12} to 10^{-8} cm^3. Within these limits, therefore, condition (17) is well satisfied already for $f \lesssim 1$ Hz, but it can be violated at larger frequencies and/or larger samples, in which cases the measured power spectrum would be *larger*, roughly by a factor of $(\hbar\omega D\Omega)^2$.

The low-frequency asymptotics of the corrected propagator and interaction vertices will be obtained in the next section, and then used in Sec. III C to extract the low-frequency asymptotic of $S_F(f)$.

B. Low-frequency phonon corrections to the propagator and interaction vertices of charge carriers

On account of the charge-carrier interactions, its propagator is modified according to

$$D_0^{(ij)}(p) \to \mathcal{D}_0^{(ij)}(p) = D_0^{(ij)}(p) + D_0^{(ik)}(p)\sigma^{(kl)}(p)\mathcal{D}_0^{(lj)}(p), \tag{18}$$

where $\sigma^{(kl)}(p)$ is the charge-carrier self-energy, and summation over repeated indices is implied [25,29,30]. This Dyson equation is to be resolved with respect to $\mathcal{D}_0^{(ij)}$, and in general, the resulting expressions are rather complicated because each component of $\mathcal{D}_0^{(ij)}$ involves $\sigma^{(kl)}$ with all pairs of indices k, l. But since $D_0^{(12)} = 0$, the off-diagonal components of $\sigma^{(ij)}$ do not contribute to the components $\mathcal{D}_0^{(11)}$, $\mathcal{D}_0^{(22)}$ which only appear in Fig. 2. Each of these thus depends only on the respective component of the self-energy, and Eq. (18) is easily solved to give

$$\mathcal{D}_0^{(11)}(p) = \frac{i}{p^0 - \varepsilon_{\boldsymbol{p}} - \sigma(p) + i0}$$

and similarly for $\mathcal{D}_0^{(22)}$, where $\sigma(p) \equiv \sigma^{(11)}(p)$ is the usual Feynman self-energy of the charge carrier. In the second order of perturbation theory, it is represented by the diagram shown in Fig. 3(a), and a similar diagram in which the solid line is replaced by a dashed line. The two interaction vertices in this diagram are of the same type: both are either (1) or (2), according to the type of the charge-carrier propagator which the self-energy correction refers to. Although its external lines are off the charge-carrier mass shell, the pole position of the inner charge-carrier propagator in Fig. 3(a) does matter,

because the energy-momentum exchange with phonons can move the charge carrier on the mass shell. The effect of virtual phonons on the charge-carrier propagation thus depends on the charge-carrier state filling (the mean occupation number v; cf. Sec. III A). The vacuum (empty band) contribution of Fig. 3(a) reads

$$\sigma_{\text{vac}}(q+k) = \frac{i}{\rho_0} \int \frac{d^3\boldsymbol{l}}{(2\pi)^3} \int_{-\infty}^{+\infty} \frac{dl^0}{2\pi} \frac{|M_\lambda(\tilde{\boldsymbol{l}})|^2}{[(l^0)^2 - \omega_l^2 + i0][q^0 + k^0 + l^0 - \varepsilon_{q+k+l} + i0]}. \quad (19)$$

This integral is nonanalytic at $k^0 = 0$, and it is this nonanalyticity that contributes to the frequency exponent deviation. In the case of parabolic dispersion of the charge-carrier energy, $\varepsilon_q = \varepsilon_0 + \boldsymbol{q}^2/2m$, where ε_0 is an arbitrary constant, the integration is elementary, though the resulting expression is rather cumbersome [28]. In contrast, its part containing the nonanalytic contribution can be rendered far more compact, and can be simply extracted as follows (similar integrals below which represent corrections to the interaction vertices are easily dealt with in the same way). First, integration over l^0 is done by taking the residue of the integrand at $l^0 = -\omega_l$. The $\boldsymbol{l}$ integral is customarily simplified by replacing $|M_\lambda(\tilde{\boldsymbol{l}})|^2$ with its angular mean, M_λ^2. Neglecting also the photon momentum $\boldsymbol{k}$ in comparison to that of the charge carrier yields

$$\sigma_{\text{vac}}(q+k) = \frac{1}{2u\rho_0} \int \frac{d^3\boldsymbol{l}}{(2\pi)^3} \frac{M_\lambda^2}{|\boldsymbol{l}|(k^0 - u|\boldsymbol{l}| - \boldsymbol{q}\cdot\boldsymbol{l}/m - \boldsymbol{l}^2/2m + i0)}. \quad (20)$$

The nonanalytic contribution comes from integration over small phonon momenta. Therefore, the term $\sim\boldsymbol{l}^2$ in the denominator can be neglected, whereupon the integral is easily done. The result can be written as

$$\sigma_{\text{vac}}(q+k) = \frac{M_\lambda^2}{(2\pi)^2 \rho_0 u (u^2 - v_q^2)} k^0 \ln \frac{|k^0|}{l_m u} + \sigma_0, \quad v_q \equiv \frac{|\boldsymbol{q}|}{m},$$

where σ_0 is the contribution of finite $\boldsymbol{l}$'s, hence, analytical at $k^0 = 0$, and l_m is an auxiliary dividing momentum. l_m is conveniently defined by the condition that the expansion of σ_0 in powers of k^0 has no linear term. σ_0 can then be omitted, because $\sigma_0|_{k^0=0}$ amounts merely to a redefinition of the parameters ε_0, m, whereas $O((k^0)^2)$ terms in σ_0 are irrelevant in the low-frequency limit. Moreover, l_m can be evaluated as $2\pi/d$, d denoting the lattice constant. This is because the contribution of finite $\boldsymbol{l}$'s to the self-energy integral is only logarithmic. Therefore, within the logarithmic accuracy, l_m may be set equal to the maximal phonon momentum in the first Brillouin zone.

The state-dependent contribution to the charge-carrier self-energy is obtained by replacing $1/(p_0 - \boldsymbol{p}^2/2m + i0)$ with $2\pi iv(\boldsymbol{p})\delta(p_0 - \boldsymbol{p}^2/2m)$ in the integrand of Eq. (19), where $v(\boldsymbol{p})$ is the mean occupation number of the state with momentum $\boldsymbol{p}$. Since the singular contribution is due to integration over $\boldsymbol{l} \to 0$, the factor $v(\boldsymbol{p})$ can be replaced by $v(\boldsymbol{q})$, and the integral is then done just as easily as before. The total self-energy is thus

$$\sigma(q+k) = \frac{(1 - 2v(\boldsymbol{q}))M_\lambda^2}{(2\pi)^2 \rho_0 u (u^2 - v_q^2)} k^0 \ln \frac{|k^0|}{l_m u}. \quad (21)$$

The interaction with phonons affects electromagnetic interactions of the charge carriers as well. The lowest-order vertex correction is drawn in Fig. 3(b), and its evaluation is quite similar to that just performed for the self-energy. The result is that when a charge carrier with momentum q on the mass shell exchanges momentum k with the electromagnetic field, the interaction vertex is multiplied by $[1 + \Gamma(q, k)]$, where

$$\Gamma(q, k) = \frac{M_\lambda^2(2v(\boldsymbol{q}) - 1)}{(2\pi)^2 \rho_0 u (u^2 - v_q^2)} \ln \frac{|k^0|}{l_m u}. \quad (22)$$

It is not difficult to check that in the diagrams of Fig. 2 this correction to any of the two side vertices just cancels the contribution (21) to the charge-carrier propagator connecting it to the central vertex. The phonon correction to the central vertex itself is slightly different from Eq. (22), for the charge-carrier lines attached to it are both off the mass shell,

$$\begin{aligned}
&\Gamma(q+k, k') \\
&= \frac{M_\lambda^2(2v(\boldsymbol{q}) - 1)}{(2\pi)^2 \rho_0 u (u^2 - v_q^2)} \\
&\quad \times \left(\ln \frac{|k^0 + k'^0|}{l_m u} + \frac{k^0}{k'^0} \ln \left| 1 + \frac{k'^0}{k^0} \right| \right) \\
&= \frac{M_\lambda^2(2v(\boldsymbol{q}) - 1)}{(2\pi)^2 \rho_0 u (u^2 - v_q^2)} \\
&\quad \times \left(\ln \frac{|k^0 + k'^0|}{l_m u} + 1 - \frac{1}{2}\frac{k'^0}{k^0} + \frac{1}{3}\left(\frac{k'^0}{k^0}\right)^2 + \cdots \right).
\end{aligned}$$

However, the additional terms do not change the general structure of the low-frequency asymptotic of $S_F(f)$, giving rise only to relatively small corrections to its magnitude. On the other hand, the logarithmic term is important as it alters the analytical structure of Feynman integrals.

Denoting

$$\delta(\boldsymbol{q}) = \frac{M_\lambda^2(1 - 2v(\boldsymbol{q}))}{(2\pi)^2 \rho_0 u (u^2 - v_q^2)}, \quad (23)$$

the product of the factor $[1 + \Gamma(q+k, k')]$ with the propagator $D(q+k+k')$ can be rewritten, within the second-order accuracy, as

$$\begin{aligned}
&[1 + \Gamma(q+k, k')]D_0^{(11)}(q+k+k') \\
&= i\frac{1 - \delta(\boldsymbol{q}) \ln \frac{|k^0+k'^0|}{l_m u}}{k^0 + k'^0 + i0} = \frac{i}{(k^0 + k'^0 + i0)} \left| \frac{l_m u}{k^0 + k'^0} \right|^{\delta(\boldsymbol{q})}.
\end{aligned}$$

It can be shown that the latter expression is actually the true infrared asymptotic of the charge-carrier propagator.

C. Low-frequency asymptotic of the power spectrum

Using the result of Sec. III B and applying Schwinger-Keldysh rules to the diagrams in Fig. 2, their contribution to the function $S(\tau) = \langle \widehat{\Delta U}(t' + \tau)\widehat{\Delta U}(t')\rangle_-$ takes the form

$$
S(\tau) = \frac{i(4\pi e^2)^2 \mathbf{E}^2}{2m}\frac{\partial^2}{\partial\lambda\partial\lambda'}\int \frac{d^4k}{(2\pi)^4}\frac{d^3\mathbf{q}}{(2\pi)^3}\frac{d^3\mathbf{q}'}{(2\pi)^3}\varrho(\mathbf{q},\mathbf{q}')[e^{i\mathbf{k}\cdot(\mathbf{x}_1-\mathbf{x}_2)}-1]e^{i(\mathbf{q}-\mathbf{q}')\cdot\mathbf{x}_1}
$$

$$
\times \left\{ e^{-ik^0\tau-ik'^0 t}G^{(11)}(q-q'+k+k')D^{(11)}(q+k+k')\left|\frac{l_m u}{k^0+k'^0}\right|^{\delta(\mathbf{q})}D^{(11)}(q+k)G^{(12)}(k)\right.
$$

$$
- e^{ik^0\tau-ik'^0 t'}G^{(21)}(k)D^{(22)}(q'-k)\left|\frac{l_m u}{k^0+k'^0}\right|^{\delta(\mathbf{q}')}D^{(22)}(q'-k-k')G^{(22)}(q-q'+k+k')
$$

$$
+ e^{-ik^0\tau-ik'^0 t}G^{(12)}(k)D^{(11)}(q'-k)\left|\frac{l_m u}{k^0+k'^0}\right|^{\delta(\mathbf{q}')}D^{(11)}(q'-k-k')G^{(11)}(q-q'+k+k')
$$

$$
\left. - e^{ik^0\tau-ik'^0 t'}G^{(22)}(q-q'+k+k')D^{(22)}(q+k+k')\left|\frac{l_m u}{k^0+k'^0}\right|^{\delta(\mathbf{q})}D^{(22)}(q+k)G^{(21)}(k)\right\}\Bigg|_{\lambda=\lambda'=0} + (\mathbf{x}_1 \leftrightarrow \mathbf{x}_2), \quad (24)
$$

where "$+(\mathbf{x}_1 \leftrightarrow \mathbf{x}_2)$" means that the preceding expression is to be added with $\mathbf{x}_1$ and $\mathbf{x}_2$ interchanged. This Fourier decomposition is only valid for an odd-in-τ part of $S(\tau)$; its part symmetric under $t \leftrightarrow t'$ is kept for a while for notational simplicity, but it will be eventually omitted. It is not difficult to see that as long as $\delta(\mathbf{q}) < 1$, λ differentiations of factors $\exp(-ik'^0 t)$, $\exp(-ik'^0 t')$ in the integrand give rise to symmetric terms which are to be omitted. The leading low-frequency term in $S_F(f)$ corresponds to contributions in which $\partial^2/\partial\lambda\partial\lambda'$ acts on the charge-carrier propagators $D^{(11)}(q \pm k \pm k')$, $D^{(22)}(q \pm k \pm k')$, because these approach their poles as $k^0 \to 0$. Since in practice $\delta(\mathbf{q}) \ll 1$, the infrared correction factors may be left undifferentiated. By virtue of $|\mathbf{k}| = |k^0|$, one has $\varepsilon_{\mathbf{q}+\mathbf{k}} = \varepsilon_{\mathbf{q}} + |k^0|O(|\mathbf{q}|/m)$, and therefore, in the nonrelativistic limit, $D^{(11)}(q+k+k') = i/(q^0 + k^0 + \lambda + \lambda' - \varepsilon_{\mathbf{q}+\mathbf{k}}) \approx i/(k^0 + \lambda + \lambda')$. Expanding also $e^{i\mathbf{k}\cdot(\mathbf{x}_1-\mathbf{x}_2)}$ to second order and performing integration over $\mathbf{k}$ gives

$$
S(\tau) = \frac{8e^4\mathbf{E}^2(\mathbf{x}_1-\mathbf{x}_2)^2}{3m}\int_0^\infty dk^0 \frac{e^{ik^0\tau}}{k^0}\int \frac{d^3\mathbf{q}}{(2\pi)^3}\frac{d^3\mathbf{q}'}{(2\pi)^3}\varrho(\mathbf{q},\mathbf{q}')\left(\left|\frac{l_m u}{k^0}\right|^{\delta(\mathbf{q})}+\left|\frac{l_m u}{k^0}\right|^{\delta(\mathbf{q}')}\right)\frac{e^{i(\mathbf{q}-\mathbf{q}')\cdot\mathbf{x}_1}+e^{i(\mathbf{q}-\mathbf{q}')\cdot\mathbf{x}_2}}{(\mathbf{q}-\mathbf{q}')^2}. \quad (25)
$$

It is now easy to check that similar transformations of the Schwinger-Keldysh integrals corresponding to the basic diagram in Fig. 1(b) yield expressions which pairwise cancel each other (this is because these diagrams involve an odd number of the charge-carrier propagators, which makes the sign of their contributions alternate).

We observe that the frequency integral in the antisymmetric part of $S(\tau)$ is convergent, provided that $\delta < 1$, namely,

$$
\int_0^\infty dk^0 \frac{\sin(k^0\tau)}{|k^0|^{1+\delta}} = -\chi(\tau)|\tau|^\delta \sin\left(\frac{\pi\delta}{2}\right)\Gamma(-\delta), \quad (26)
$$

where $\chi(x) = x/|x|$, and $\Gamma(x)$ is the Euler function. The obtained expression is to be substituted into the right-hand side of Eq. (6). One has

$$
\int_{-t_m}^{t_m} d\tau\, \chi(\tau)|\tau|^\delta e^{i\omega\tau} = 2i\chi(\omega)\cos\left(\frac{\pi\delta}{2}\right)\int_0^{t_m} dx\, x^\delta e^{-|\omega|x} - \frac{2it_m^\delta}{\omega}\cos(\omega t_m) + O(t_m^{\delta-1}),
$$

$$
\frac{1}{t_m}\int_{-t_m}^{t_m} d\tau\, \tau|\tau|^\delta e^{i\omega\tau} = -\frac{2it_m^\delta}{\omega}\cos(\omega t_m) + O(t_m^{\delta-1}).
$$

We thus see that despite that these expressions diverge in the limit $t_m \to \infty$, their difference does converge to a finite value:

$$
\lim_{t_m\to\infty}\left\{\int_{-t_m}^{t_m} d\tau\, \chi(\tau)|\tau|^\delta e^{i\omega\tau} - \frac{1}{t_m}\int_{-t_m}^{t_m} d\tau\, \tau|\tau|^\delta e^{i\omega\tau}\right\}
$$

$$
= 2i\chi(\omega)|\omega|^{-1-\delta}\cos\left(\frac{\pi\delta}{2}\right)\Gamma(1+\delta). \quad (27)
$$

In practice, the voltage probes are usually aligned parallel to $\mathbf{E}$ (the noise measured in this configuration is sometimes called longitudinal). In this case, $\mathbf{E}^2(\mathbf{x}_1-\mathbf{x}_2)^2 = U_0^2$. The remaining momentum integrals are conveniently evaluated by expressing $\varrho(\mathbf{q},\mathbf{q}')$ via the mixed position-momentum

distribution function according to Eq. (16). Since $R(\mathbf{r},\mathbf{Q})$ vanishes for $\mathbf{r}$ outside of the sample, $(\mathbf{q}'-\mathbf{q}) = \mathbf{p}$ is of the order of the inverse linear sample size which in practice is much larger than the lattice constant. Therefore, $|\mathbf{p}| \ll |\mathbf{q}|$ for all relevant charge-carrier momenta, so that $(1/|\mathbf{q}| + 1/|\mathbf{q}'|) \approx 2/|\mathbf{Q}|$. The integral over $\mathbf{p} = \mathbf{q}' - \mathbf{q}$ in Eq. (25) is then just a Fourier decomposition of the Coulomb potential. In view of the assumed macroscopic sample homogeneity, $R(\mathbf{r},\mathbf{Q}) = R(\mathbf{Q})$ within the sample, where $R(\mathbf{Q})$ is normalized by

$$
\int \frac{d^3\mathbf{Q}}{(2\pi)^3}R(\mathbf{Q}) = 1.
$$

Combining Eqs. (25)–(27) and restoring cgs units, the low-frequency asymptotic of the power spectrum finally takes the form

$$S_F(f) = \frac{2e^4 g}{\pi m \hbar c^3} \frac{U_0^2}{|f|} \int \frac{d^3 \boldsymbol{q}}{(2\pi\hbar)^3} R(\boldsymbol{q}) \left| \frac{f_*}{f} \right|^{\delta(\boldsymbol{q})}, \qquad (28)$$

where

$$\delta(\boldsymbol{q}) = \frac{(1 - 2\nu(\boldsymbol{q}))M_\lambda^2}{(2\pi)^2 \hbar \rho_0 u (u^2 - v_q^2)}, \quad f_* = \frac{u}{d}, \qquad (29)$$

and g is a geometrical factor (it is defined following Ref. [17]):

$$g = \frac{1}{3\Omega} \int_\Omega d^3 \boldsymbol{r} \left(\frac{1}{|\boldsymbol{r} - \boldsymbol{x}_1|} + \frac{1}{|\boldsymbol{r} - \boldsymbol{x}_2|} \right).$$

In some experiments, however, the voltage probes are located differently. In the rather rare case of $(\boldsymbol{x}_1 - \boldsymbol{x}_2)$ perpendicular to $\boldsymbol{E}$, the so-called transverse noise is measured. Specifically, if the current leads and voltage probes are attached to the surface of a rectangular film of length l and width w, then $|\boldsymbol{x}_1 - \boldsymbol{x}_2| = w$, $|\boldsymbol{E}| l = U_0$, so that the factor g in Eq. (28) is to be replaced by

$$g^{\text{tr}} = \left(\frac{w}{l} \right)^2 \frac{1}{3\Omega} \int_\Omega d^3 \boldsymbol{r} \left(\frac{1}{|\boldsymbol{r} - \boldsymbol{x}_1|} + \frac{1}{|\boldsymbol{r} - \boldsymbol{x}_2|} \right). \qquad (30)$$

It follows from Eq. (28) that because of the dependence of δ on the charge-carrier momentum, the voltage power spectrum is a superposition of many $1/f^\gamma$ contributions with different γ's. Numerical evaluation of the integral in Eq. (28) reveals that despite this complication, it is perfectly well approximated as $|f_*/f|^{\bar{\delta}}$ with some $\bar{\delta}$, so that

$$S_F(f) = \frac{2e^4 g}{\pi m \hbar c^3} \frac{U_0^2}{|f|^{\bar{\gamma}}} f_*^{\bar{\gamma}-1}, \qquad (31)$$

where $\bar{\gamma} = 1 + \bar{\delta}$ is an effective frequency exponent. This is illustrated in Fig. 4 where the right-hand side of Eq. (28) is plotted in the simplest case of $R(\boldsymbol{q}) \sim N(\varepsilon(\boldsymbol{q}))$, with $N(\varepsilon) = [\exp(\varepsilon - \mu)/T + 1]^{-1}$ the Fermi distribution, for various values of temperature T and chemical potential μ. The strength of the electron-phonon coupling can be quantified by the parameter $M_\lambda^2/(2\pi)^2 \hbar \rho_0 u^3$ (equal to 0.1 in the figure), which is the value of $\delta(\boldsymbol{q})$ for $\boldsymbol{q} = 0$ and vanishing mean occupation number. The apparent pole of $\delta(\boldsymbol{q})$ at $v_q = u$ is a result of neglecting the term $\sim l^2$ in Eq. (20) when extracting the nonanalytic contribution. This simplification is justified for all $\boldsymbol{q}$ except in a very small vicinity of $|\boldsymbol{q}| = mu$, where the integral actually has a branch point and is finite. The width of this region $\Delta|\boldsymbol{q}| \sim \sqrt{m\hbar f} \to 0$ as $f \to 0$; therefore, its contribution to the integral in Eq. (28) can be discarded, because it does not affect the leading low-frequency term of $S_F(f)$. It is seen from Fig. 4 that $\delta(0)$ is just a characteristic variation of the effective frequency exponent with respect to variations in the charge-carrier temperature and chemical potential. The corresponding variation of the power spectrum at 1 Hz is on the order of $(f_*/1\,\text{Hz})^{\delta(0)} = 10^{1.4} \approx 25$.

We conclude that the power spectrum of fundamental noise is of the form typical of the observed flicker noise: it is a power law in frequency and is quadratic with respect to the voltage bias. At last, it is to be recalled that these results, including expression (29), are valid under the condition of
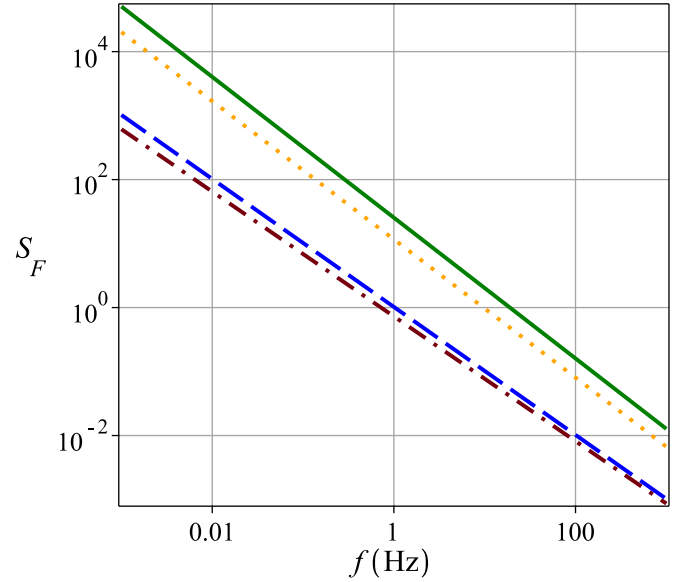

FIG. 4. Power spectrum (arbitrary units) versus frequency as given by Eq. (28) with $f_* = 10^{14}$ Hz, m the free electron mass, $u = 10^6$ cm/s, and all other physical parameters chosen so that $M_\lambda^2/(2\pi)^2 \hbar \rho_0 u^3 = 0.1$, for $T = 0.01$ K, $\mu/T = -10$ (solid, $\bar{\gamma} = 1.10$), $T = 0.01$ K, $\mu/T = -1$ (dotted line, $\bar{\gamma} = 1.08$), $T = 300$ K, $\mu/T = 10$ (dashed line, $\bar{\gamma} = 1.0$), $T = 300$ K, $\mu/T = -15$ (dash-dotted line, $\bar{\gamma} = 0.975$), where $\bar{\gamma}$ is the line slope as read off directly from the plot.

no acoustic reflection at the current leads. Though this is the relevant condition for low-frequency phonons, we note that in the opposite case of complete acoustic reflection, the long-wavelength phonon modes would be cut off, so that $\delta(\boldsymbol{q}) = 0$.

IV. COMPARISON WITH EXPERIMENT

The existence of a quantum bound on the voltage power spectrum naturally raises the question of its practical attainability. It is to be noted, first of all, that there are two fundamental reasons why this bound cannot be strictly attained experimentally even in perfectly clean samples. A formal reason is that this might happen only in a state which is an eigenstate of the operator

$$\widehat{\Delta U_c}(\omega) + i\widehat{\Delta U_s}(\omega) = \int_0^{t_m} dt \, \widehat{\Delta U}(t) e^{i\omega t}, \qquad (32)$$

as can be easily inferred from Eq. (3) and the fact that $S_F(f)$ is the minimum of $S(f)$. But such eigenstates are of infinite norm, because the spectrum of $\widehat{\Delta U}(t)$ is continuous. Furthermore, the voltage measurement entails the system state variations such that ΔU at each instant are found in a more or less narrow range of values dependent on the measurement accuracy. The system state is thus driven over states which are closer to eigenstates of the operator $\widehat{\Delta U}(t)$, rather than to those of Eq. (32).

The other, practical reason why the observed power spectra cannot be arbitrarily close to the quantum bound is the back-action of the voltage measurements on the currents flowing in the conductor. In addition to the direct influence of the voltage measurement on the electromagnetic field state, dis-

cussed so far, interaction with the measuring apparatus also alters the system state in the charge-carrier sector. Namely, a perturbation in the electric current caused by the voltage measurement at some instant will affect the voltages at later times and, hence, also the voltage power spectrum. Since it is due to a purely electromagnetic interaction between the charge carriers and the measuring apparatus, this effect is formally of the same (sixth) order with respect to the elementary charge as that of the direct charge-carrier collisions via their Coulomb interaction. As such, therefore, it is not captured by the lowest-order approximation used throughout, and so the presence of these perturbations implies that the observed noise power will be higher than predicted. It can be mentioned in this connection that on the practical side, there is another important source of uncertainty in measuring the power spectrum, which is related to determination of the static bias voltage used in the definition of the voltage fluctuation. This voltage is itself an estimated quantity, and care must be taken in the signal processing in order to ensure that its error does not affect the power spectrum (e.g., resetting the mean value of the signal to a predetermined constant prior to each data-collecting run, or removing a constant mean after "prewhitening" the data; the latter also helps to reduce the variance of the experimental power spectrum estimate [6]). At the same time, since the lower bound on the power spectrum is determined by an odd-in-τ contribution to $S(\tau)$, it is insensitive to the voltage mean used in the definition of $\widehat{\Delta U}(t)$. Since the voltage variance takes on its minimum value when evaluated using the true mean, it follows that errors in the static bias amplify the measured noise power, hence its deviation from the lower bound.

Thus, it appears that the observed spectral powers of $1/f$ noise should markedly exceed the bound set by quantum indeterminacy. On the other hand, the task of minimization of the measurement influence on the system under study has always been an essential part of any experimental strategy. This suggests that the noise levels observed in sufficiently clean samples upon elimination of the conventional noise sources can be expected to be not very far from the lower bound. To see how far they actually are from the value (28), we consider below several typical cases which are also quite revealing on their own with regard to the problems they pose to the traditional view on the flicker noise as originating from the conductance fluctuations.

A. Time dependence of the voltage variance

It has been experimentally established that the voltage variance grows roughly logarithmically with the measurement time [8,31,32]. The present approach does not allow an explicit calculation of the voltage variance, because what is left of the function $\langle \widehat{\Delta U}(t)\widehat{\Delta U}(t')\rangle$ at $t' = t$ is its symmetric part which was discarded in the above considerations. Yet, an asymptotic growth of the voltage variance at large times can be described indirectly as follows. Consider first the case of a pure $1/f$ noise, $S_F(f) = A/|f|$, where $A > 0$ is a constant dependent on the sample properties. One has $S(f) \geqslant S_F(f)$, and, as we just argued, the last inequality is actually a strict one. Next, we note that a $1/|\omega|$ asymptotic of the power spectrum suggests that at large $|\tau|$'s, $S(\tau)$ contains a term $\sim \ln|\tau|$.

In fact, in a perfect analogy to the derivation of Eq. (27), but this time for an even-in-τ part of $S(\tau)$, one finds

$$\int_{-t_m}^{t_m} d\tau \ln|\tau| e^{i\omega\tau} = -\frac{\pi}{|\omega|} - 2\ln t_m \frac{\sin(\omega t_m)}{\omega} + O(1/t_m),$$

$$\frac{1}{t_m}\int_{-t_m}^{t_m} d\tau |\tau| \ln|\tau| e^{i\omega\tau} = -2\ln t_m \frac{\sin(\omega t_m)}{\omega} + O(1/t_m),$$

so that the power spectrum for $S(\tau) = \ln|\tau|$ converges to $-\pi/|\omega|$. It is also straightforward to check that an additive constant in $S(\tau)$ does not contribute to the power spectrum. It follows that in order to have a low-frequency asymptotic $A/|f|$ of the power spectrum, the symmetric part of $S(t - t') = \langle \widehat{\Delta U}(t)\widehat{\Delta U}(t')\rangle_-$ must have a large-time asymptotic $(-2A)\ln(|\tau|/\tau_0)$, where $\tau_0 > 0$ is an arbitrary constant. As discussed at length in Ref. [17], the notion of autocorrelation is not well defined, because in a given system state, $\Delta U(t)$ cannot have definite values at different times. But the fact that $S(\tau)$ grows with τ implies that the observable $[\hat{U}(t) - \hat{U}(t')]$ is smeared over a range of values which also grows with τ, at least as $\sqrt{|S(\tau)|}$. Therefore, the symmetric variance

$$\sigma_U = \frac{1}{2}[\langle \widehat{\Delta U}^2(t)\rangle + \langle \widehat{\Delta U}^2(t')\rangle]$$

must grow at least as $|S(\tau)|$. More formally, this follows from the inequality

$$0 \leqslant \langle [\widehat{\Delta U}(t) + \widehat{\Delta U}(t')]^2\rangle = \langle \widehat{\Delta U}^2(t)\rangle + \langle \widehat{\Delta U}^2(t')\rangle$$
$$+ \langle \widehat{\Delta U}(t)\widehat{\Delta U}(t')\rangle + \langle \widehat{\Delta U}(t')\widehat{\Delta U}(t)\rangle.$$

Thus, $\sigma_U \geqslant 2A\ln(|\tau|/\tau_0)$ at large τ. If one of the time arguments is kept fixed, say, $t' = 0$, then this result can be rewritten for the voltage variance at time $t > 0$ as

$$\langle \widehat{\Delta U}^2(t)\rangle = B\ln\left(\frac{t}{\tau_0}\right), \qquad (33)$$

where $B = \text{const} \times A$, with a number of order unity as the proportionality constant.

Quite similarly, in the case of $1/f^\gamma$ noise, one finds

$$\langle \widehat{\Delta U}^2(t)\rangle = Ct^{\gamma-1} + D, \qquad (34)$$

where C and D are some constants. Since adding a constant to $S(\tau)$ does not change $S(f)$, the value of D cannot be deduced from the power spectrum itself. In principle, it is to be found by calculating the symmetric part of $S(\tau)$ explicitly, a task which is avoided by the present approach. Empirically, D is determined, together with the other parameters, from best fits of Eq. (34) to the experimental data. An example is given in Fig. 5.

B. Noise in InGaAs quantum wells

1. Longitudinal noise

As a second example, we take Ref. [10] reporting noise measurements in $\text{In}_{1-x}\text{Ga}_x\text{As}$ quantum wells of significantly different sizes. The charge carriers in this case are electrons (n) and holes (p). Since $\varkappa \sim 1/m$, it is sufficient to consider the lightest charge carriers whose masses are $m_n = 0.06m_0$ and $m_p = 0.09m_0$, respectively, where m_0 is the free electron mass (these are approximate values, as the masses depend on the sample thickness, composition, etc.). As was discussed in
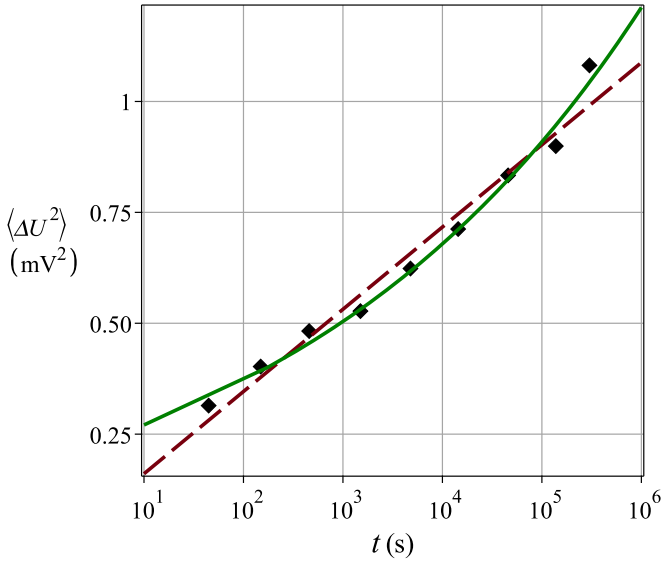
FIG. 5. Voltage variance versus time as read off from Fig. 5 of Ref. [8] (marks, the experimental uncertainty was not specified), and fitted using Eq. (33) with $B = 0.0805$ mV^2, $\tau_0 = 1.36$ s (dashed line, the residual standard deviation is 0.05 mV^2) and Eq. (34) with $C = 0.24$ mV^2 s$^{-0.12}$, $D = -0.047$ mV^2, $\gamma - 1 = 0.12$ (solid line, the residual standard deviation is 0.03 mV^2).

the Introduction, there is a strong correlation between δ and the noise magnitude. In terms of calculational uncertainty this means that the theoretical value of $S(f)$ is rather sensitive to the error in δ. In the present case, an experimental error in δ is around 0.03 [33]. Taking into account that in InGaAs, $d \approx 5 \times 10^{-8}$ cm, $u = (2.5–5) \times 10^5$ cm/s, one finds that this error gives rise to a factor of $(f_*)^{0.03} \approx 10^{13 \times 0.03} \approx 2.5$ in the noise magnitude. Yet, the error in a theoretical estimate of δ is even larger. By this reason, when comparing Eq. (31) with the experiment, the measured values of γ are used in place of the effective frequency exponent $\bar{\gamma}$. Table I compares, in terms of the reduced power spectrum $\varkappa = S(f)f^\gamma/U_0^2$, the theory with the experimental data taken from Figs. 4–7 of Ref. [10]. In cases where the measured spectra have the frequency exponent equal to unity within the experimental error, they are compared to Eq. (31) with $\bar{\gamma} = 1$. In the instances where $|\gamma - 1|$ exceeds the experimental error, two values of

$\varkappa$ are given in the table: one is calculated for the measured γ, and the other for $\gamma = 1$. We observe that in all samples, the measured $\varkappa$ is no more than an order of magnitude larger than the calculated. Notably, in sample V5, this is brought about by the effect of $\gamma \neq 1$ which increases $\varkappa_{\text{th}}$ fivefold. In sample V2, on the contrary, the effect is to decrease $\varkappa_{\text{th}}$ so that the ratio $\varkappa_{\text{expt}}/\varkappa_{\text{th}}$ becomes some four times. Taking into account the calculational accuracy and also what was said at the beginning of Sec. IV with regard to attainability of the quantum bound, these observations lead us to conclude that the observed noise levels are nearly minimal.

At last, it is instructive to estimate theoretically the maximum of $|\gamma - 1|$, which is well quantified by the value of $\delta(0)$ (cf. the end of Sec. III C). M_λ^2 is customarily evaluated as $(eh_{14})^2$, where the piezoelectric constant $h_{14} = -1.4 \times 10^9$ V/m. The lowest acoustic wave velocity, $u = 2.5 \times 10^5$ cm/s, is for propagation in the direction [110]; substitution of these figures together with $\rho_0 = 5.3$ g/cm^3 in Eq. (29) gives $\delta(0) = 0.14$. The figures used are for samples with low indium fraction; in the case $x = 0.47$ (which is of special interest for microelectronics as it provides the best electron mobility and other characteristics of single crystals), $\delta(0)$ drops to 0.09.

2. Transverse noise

Reference [10] is one of a handful of papers that deal with the transverse noise, that is, voltage fluctuations in a direction perpendicular to the current flow in the sample [34–36]. Within the conventional model of flicker noise as originating from the conductance fluctuations, the theory (based on a phenomenological inclusion of the term $1/f$ into the fluctuation spectrum) predicts that for a given electric field, the power spectrum is independent of the distance $|\boldsymbol{x}_1 - \boldsymbol{x}_2|$ between the voltage probes [36]. On the other hand, according to the present theory, $S_F(f)$ is proportional to this distance squared [cf. Eq. (25)]. The computed and measured values of $\varkappa$ are summarized in Table II. First of all, a sample-to-sample comparison of the last columns in Tables I and II reveals that the observed levels of transverse noise in all cases are significantly lower than the corresponding levels of the longitudinal noise. Second, it is seen that the reduction by a factor of $(w/l)^2$ predicted by Eq. (30), which varies in the range 1/16 to 1/4, brings $\varkappa_{\text{th}}$ to values which are roughly in the same ratios to the measured values as in the case of longitudinal

TABLE I. Reduced power spectra of flicker noise as measured in Ref. [10] ($\varkappa_{\text{expt}}$) and calculated according to Eq. (31) ($\varkappa_{\text{th}}$) for various InGaAs heterostructures. Top values in braces are for $\gamma = 1$; bottom values are for measured γ, and are the ones to be compared with $\varkappa_{\text{expt}}$. The calculational uncertainty in $\varkappa_{\text{th}}$ is a factor of 2.5 (see the text), whereas uncertainty in $\varkappa_{\text{expt}}$ estimated from the vertical spread of the measured power spectra is a factor of 2 [33]. Also given are the quantum well dimensions [width (w), length (l), and thickness (a)] and the corresponding value of geometrical factor g. Uncertainties in these parameters ($\sim$10%) are negligible in the total uncertainty of $\varkappa_{\text{th}}$.

Sample	w (μm)	l (μm)	a (nm)	g (cm^{-1})	γ	$\varkappa_{\text{th}}$ (Hz$^{\gamma-1}$)	$\varkappa_{\text{expt}}$ (Hz$^{\gamma-1}$)
V1	1	2.2	10	9630	1	3.5×10^{-10}	1.75×10^{-9}
V1.5	1.5	3.3	10	6420	1	2.3×10^{-10}	4.5×10^{-10}
V2	2	4	10	5140	0.97	$\begin{cases} 1.7 \times 10^{-10} \\ 6.9 \times 10^{-11} \end{cases}$	3.1×10^{-10}
V5	5	20	20	1260	1.05	$\begin{cases} 4.4 \times 10^{-11} \\ 2.1 \times 10^{-10} \end{cases}$	1.5×10^{-9}
V80	80	300	20	80	1	1.9×10^{-12}	4.1×10^{-12}

TABLE II. Same as in Table I, but for transverse noise.

Sample	g^{tr} (cm^{-1})	γ	$\varkappa_{\mathrm{th}}$ (Hz$^{\gamma-1}$)	$\varkappa_{\mathrm{expt}}$ (Hz$^{\gamma-1}$)
V1	2310	1	7.2×10^{-11}	2.4×10^{-10}
V1.5	1540	1	5.1×10^{-11}	1.3×10^{-10}
V2	1310	0.96	$\begin{cases} 4.3 \times 10^{-11} \\ 1.3 \times 10^{-11} \end{cases}$	3.9×10^{-11}
V5	100	1.05	$\begin{cases} 3.3 \times 10^{-12} \\ 1.5 \times 10^{-11} \end{cases}$	7.5×10^{-11}
V80	7	1	2.5×10^{-13}	3.9×10^{-13}

noise. The general conclusion regarding the observed noise magnitudes is thus the same as that drawn from Table I.

C. "Huge" noise in high-T_c superconductors

It is of considerable interest to make a similar comparison for high-temperature (high-T_c) superconductors, as they are known to exhibit anomalously high levels of $1/f$ noise. It so happened that the noise in these materials was first measured in samples of sizes unusually large for flicker noise studies—the linear sample dimensions were several millimeters [37]. Subsequent measurements in much smaller samples gave much lower noise levels though. This issue was considered in detail in Ref. [38] where it was demonstrated that the anomaly in the noise levels is spurious. Namely, it is a consequence of an inappropriate normalization of the power spectra using Hooge's formula [39] according to which $S(f) \sim 1/\Omega$, whereas actually $S(f)$ is inversely proportional to the *linear* sample size. Here we will only show in a couple of examples that the "huge" noise is in fact not far from the minimum given by Eq. (28). The results of Sec. III are applicable in this case because the charge-carrier density in the normal state of high-T_c superconductors is small compared to that in normal metals, so that the charge-carrier energy-momentum dispersion is well described in terms of the band effective mass.

The work [40] reports $1/f$-noise measurements in bulk samples of YBa$_2$Cu$_3$O$_y$. The samples used were single crystals with $l = w = 0.2$ cm, $a = 0.01$ cm. The authors give the value 1.06 ± 0.1 for the frequency exponent. The charge carriers in this case are holes. A precise determination of the hole effective mass in this material is difficult; the experiment suggests that $m_p \approx (2\text{–}3)m_0$, and that it is nearly constant in the range of y's for which the material exhibits superconductivity, that is, for sufficiently small oxygen deficiency [41,42]. In the work under consideration, such is sample B, and the value of $\varkappa$ measured near the superconducting transition is $\varkappa_{\mathrm{expt}} = 3 \times 10^{-14}$ Hz$^{0.06}$ (as deduced from Fig. 2 of Ref. [40] assuming $\delta = 0.06$; experimental uncertainty was not specified). On the other hand, Eq. (31) with $m_p = 3m_0$ yields $\varkappa_{\mathrm{th}} = 2.2 \times 10^{-14}$ Hz$^{0.06}$, with the calculational uncertainty a factor of 20 implied by the experimental error 0.1 in δ. It is worth noting that the value of the Hooge parameter found by the authors of Ref. [40] for this sample is 2.1×10^3, that is, *six* orders of magnitude higher than the canonical value 2×10^{-3} [39].

In 1994, a systematic investigation of the flicker noise in thin films of YBa$_2$Cu$_3$O$_y$ was undertaken in order to deter-

mine its dependence on the oxygen content, y [43]. The Hooge parameter was found to be ≈ 14. This is still large compared to pure metals, but several orders of magnitude lower than those reported previously for the compound, and the authors of Ref. [43] attributed this reduction to the quality of their thin films. All samples had $a = 8.5 \times 10^{-6}$ cm, $l = 0.5$ cm, $w = 0.07$ cm, and δ was found to be in the range 0–0.1. The reduced power spectrum was found to exhibit a sharp minimum at $y \approx 6.5$, where the measurements gave $\varkappa_{\mathrm{expt}} = 3 \times 10^{-15}$ Hz$^{0.05}$ (as deduced from Fig. 3 of Ref. [43] assuming $\delta = 0.05$; experimental uncertainty was not specified). On the other hand, substitution of the sample dimensions together with $m_p = 3m_0$, $\delta = 0.05$ in Eq. (31) gives $g = 6$ cm^{-1} and the theoretical minimum $\varkappa_{\mathrm{th}} = 10^{-14}$ Hz$^{0.05}$, with the calculational uncertainty a factor of 4.5.

V. DISCUSSION AND CONCLUSIONS

We have shown that on account of the charge-carrier–phonon interaction, the low-frequency asymptotic of the quantum bound on the voltage power spectrum becomes $\sim 1/f^\gamma$, where $(\gamma - 1)$ can be of either sign depending on the filling of the charge-carrier states. This asymptotic is also quadratic with respect to the voltage bias, so that it is typical of the observed flicker noise spectra.

An important outcome of our consideration is that the law $1/f^\gamma$ with $1 < \gamma < 2$ is consistent with an unbounded growth of the correlation function $S(\tau)$ at large times. Namely, the power spectrum defined by Eq. (2) does exist despite $S(\tau) \sim \tau^{\gamma-1}$, and formula (6) is the correct way to compute it in this case. Directly related to this behavior of $S(\tau)$ is the fact that the voltage variance $\langle \Delta U^2(t) \rangle$, though finite, also grows with time as $t^{\gamma-1}$. As unusual as it might appear, this growth was nonetheless demonstrated in Sec. IV A to be perfectly consistent with the assumed stationarity of physical conditions, and confirmed by the experiment.

Next, as shown in Sec. IV by comparing Eq. (31) with the experimental data, the observed noise levels are in most cases only a few times as high as the theoretical minimum, being in all cases within an order of magnitude therefrom. In view of the comparatively large uncertainty in the calculated noise levels which makes them actually order-of-magnitude estimates, a conclusion suggested by the comparison is that the noise observed in the considered experiments is nearly minimal. This does not exclude a possibility that the noise level might be somewhat lower, but was raised to the observed values by an independent measurable effect. In fact, the photon heat bath contribution to the $1/f$ noise in high-T_c superconductors at room temperature is comparable to the vacuum contribution [38].

The existing order-of-magnitude accuracy of determining the noise magnitude, which might be deemed as disastrous in other areas of science, is yet sufficient to make further important conclusions. First, a significant drop of the noise levels on switching from the longitudinal to transverse configuration, observed in Ref. [10], takes place without exception in all samples studied. This rules out the conventional interpretation of $1/f$ noise as a result of fluctuations in the sample conductivity, which predicts the same noise level in

the two configurations. On the other hand, the amount of drop is well correlated with the law $S_F(f) \sim (w/l)^2$ predicted by Eq. (30). From a more general standpoint, dependence of $S(f)$ on the sample dimensions as given by this equation naturally resolves the puzzle of inexplicably high values of noise observed in comparatively large samples. Specifically, in the case of high-T_c superconductors, the noise magnitudes in millimeter-size samples, normalized according to Hooge's formula, were found to be 10^6 to 10^{10} times as high as in micrometer-size thin films. Why samples of comparable quality are so distinct with regard to their noise levels can be explained only if one admits that the scaling $S(f) \sim 1/\Omega$ implied by Hooge's formula is incorrect. A comparison made in Sec. IV C demonstrates, on the contrary, that when analyzed on the basis of Eq. (28), the noise observed in millimeter-size high-T_c superconductors is as ordinary as in the other instances considered.

At last, in light of the presented results, it is worth to outline a possible route to empirically decide whether the flicker noise level measured in a given material is close to the quantum bound. Assuming that the contributions of conventional noise sources have been eliminated in either of the ways mentioned in the Introduction, in order to see if the remainder is the fundamental noise it is crucial to have a reliable estimate of the frequency exponent. Its experimental error can be reduced by increasing the frequency span and by accumulating experimental data. Scanning wider bandwidths is also helpful in identifying conventional noise sources, while statistical means permit establishing various trends such as the frequency exponent dependence on the charge-carrier density. Even a crude measurement of this particular dependence may give a hint as to whether the quantum indeterminacy dominates the power spectrum. In fact, a rule of thumb is that at temperatures such that the mean charge-carrier velocity markedly exceeds the sound speed (which is normally the case, e.g., at room temperature), the frequency exponent grows with the increasing charge-carrier density [cf. Eq. (29)]. This trend is reversed only at very low temperatures (cf. Fig. 4). A more detailed verification of this dependence will require careful evaluation of the momentum integral in Eq. (28), in particular, elaboration of the kinetic model to obtain a realistic charge-carrier momentum distribution. It is advantageous to use a setting where the charge-carrier density can be varied independently of temperature and separately in each sample (e.g., when the sample is part of the field effect transistor). This would allow one to exclude sample-to-sample variations in δ which are often significant, and also to check the dependence of $S(f)$ on the total number of charge carriers in the sample. Probing this dependence is another way to rule out conventional mechanisms which all predict the inverse proportionality, while the quantum bound depends on the sample dimensions rather than the number of charge carriers. On the other hand, studying the sample geometry effects is hindered by the sample-to-sample variations in δ unless the sample size variation is sufficiently large, as in the case of high-T_c superconductors discussed above.

The data that support the findings of this study are available within the article. Any further details of calculations are available from the author upon request.

APPENDIX: SOME COMMENTS ON THE QUANTUM THEORY OF $1/f$ NOISE

There are a number of statements and/or frequently asked questions regarding the quantum theory of flicker noise which exist primarily in a verbal form. They are briefly discussed and answered in this Appendix.

1. Low-frequency photons are of large spatial extent (as their wavelength c/f is much larger than the typical size of $1/f$ experimental setup), implying that the $1/f$ power spectrum should depend on everything on Earth, if the noise is somehow related to such photons

Curiously, this argument is never applied to thermal noise, although the notion of energy per one electromagnetic degree of freedom with a given frequency is used in the derivation (original as well as modern one, based on the fluctuation-dissipation theorem) of its power spectrum. In fact, a full version of the Nyquist formula which emphasizes Planck's notion of energy quantum reads

$$S(f) = \frac{4Rhf}{e^{hf/T} - 1},$$

where R is the sample resistance, and $h = 2\pi\hbar$ [44]. This reduces to the familiar $4RT$ in the case of $f \ll T/h$, but the idea of energy quanta exchange in a circuit which underlies the derivation of the power spectrum remains valid no matter how large the photon wavelength is compared to the circuit size. A misleading premise in the above statement in italic is that a photon can be assigned a "size," and that this size is equal to the photon wavelength. But it is known already from nonrelativistic quantum mechanics that the de Broglie wavelength of a particle does *not* determine the size of the region where it is smeared. The latter depends on how waves with different wavelengths are superposed, and may or may not be of the order of a characteristic wavelength. Moreover, an important specifics of the photon is that it lacks the notion of spatial probability distribution, which deprives the photon position, size, etc., of meaning altogether.

2. Charge carriers cease to radiate low-frequency photons once the experimental setup is enclosed into a Faraday cage, thus removing this mechanism from the list of possible flicker noise sources

This statement is false as the charge carriers do radiate low-frequency photons even when enclosed in a Faraday cage. This becomes evident when the system "accelerating charge plus Faraday cage" is considered at distances much larger than the cage size. It then radiates as any other accelerating charge.

3. The transit time of the charge carrier in a sample is often shorter than the inverse frequency at which the noise is detected. Therefore, the underlying process cannot be one-particle

This argument is incorrect in that it ascribes individuality to a charge carrier. A proper description of an elementary process of the noise generation mechanism considered in the present theory is that the quantized electromagnetic field interacts not with a concrete charge carrier moving over a particular path through the sample, but with the charge carriers filling a given energy eigenstate. As a result of particle collisions, the charge carriers continually undergo transitions between different states, so that the whole effect includes contributions from all possible charge-carrier states. Like any other high-frequency process, these transitions do not affect the low-frequency component of the electromagnetic field. By virtue of the indistinguishability of identical particles, it does not matter which charge carrier occupied a given state at a given instant. Of all possible information about the charge-carrier dynamics, the noise power spectrum thus depends only on the mean state occupation numbers [cf. Eqs. (28) and (29)].

4. Relation to Handel's theory

The term "quantum $1/f$ noise" is historically associated with the name of Handel, who first attempted to describe flicker noise as a purely quantum phenomenon by relating it to the infrared divergence in the coupling of electric charges to photons [45,46]. The original derivation has been amended and modified in several respects [47–52] in response to numerous severe critics, which has resulted in two different formulas for the spectral density, the so-called coherent and conventional quantum $1/f$ effects. They read, respectively,

$$S_{\mathrm{coh}}(f) = \frac{2\alpha U_0^2}{\pi |f| N}, \qquad (A1)$$

where N is the number of charge carriers in a sample, $\alpha = e^2/(\hbar c) \approx 1/137$ is the fine structure constant, and

$$S_{\mathrm{conv}}(f) = \frac{2\alpha A U_0^2}{\pi |f| N}, \quad A = \frac{2}{3}\left(\frac{\Delta \boldsymbol{v}}{c}\right)^2, \qquad (A2)$$

where $\Delta \boldsymbol{v}$ is the change of the charge-carrier velocity in a characteristic scattering process [51]. Since normally the charge carriers are nonrelativistic, $A \ll 1$.

An approach advanced in the present paper is related neither to the infrared divergences in the scattering amplitudes or propagators of the charge carriers, nor to the decoherence phenomena induced by their interaction with the environment which plays the central role in Handel's considerations. Regarding the value of the frequency exponent, a major distinction between the present approach and Handel's is that γ in the latter is actually slightly less than unity, $\gamma_H = 1 - \alpha A < 1$. This fact, though not reflected in the canonical expressions (A1) and (A2) which neglect $\alpha A \lll 1$ in the exponent, has always been emphasized by Handel himself as guaranteeing convergence of the total noise power [45,52]. On the other hand, the numerous flicker noise measurements unequivocally demonstrate that $(\gamma - 1)$ can be positive as well as negative, and as the results of the present approach show, the charge-carrier interactions with phonons lead to deviations of γ from unity which can be of either sign consistently with finiteness of the total noise power.

Another important distinction between expressions (A1) and (A2) and Eq. (28) is the factor of N in their denominators. This dependence on the number of charge carriers implies that for a fixed charge-carrier density, $S_{\mathrm{coh}}, S_{\mathrm{conv}} \sim 1/\Omega$, whereas S_F given by Eq. (28) scales in the inverse proportionality to the *linear* size of the sample (cf. expressions for the geometrical factor g in Sec. III C). By this reason, on increasing the sample size, Handel's formulas more and more underestimate the noise level, resulting in many-order discrepancies with the experiment in millimeter-size samples (cf. Sec. IV C).

5. Relation to self-organized criticality

One of the origins of $1/f$ noise in dissipative dynamical systems is the occurrence of the so-called self-organized critical states [53,54]. In these states, the system has no characteristic length scales except for its size. Local perturbations of the system in such states are therefore correlated in time by power laws, because the lack of characteristic spatial length scale naturally leads to a lack of characteristic time scale. The corresponding power spectra are thus also power laws, $S(f) \sim 1/f^\gamma$, where $0 < \gamma < 2$. As the results of the present approach show, power spectra of the voltage fluctuations have low-frequency asymptotics of the same type, which raises the question of whether these results can be interpreted in terms of self-organized criticality. This is impossible for the following reasons. Quantum indeterminacy underlying the present approach provides no such implication between the existence of spatial and temporal scales (or the absence thereof) as that assumed in the approach based on self-organized criticality. Voltage fluctuations do not involve large time scales merely because all microscopic processes are characterized by very small times, while quantum indeterminacy itself has no intrinsic time scale. Consequently, the system need not be in a critical state to exhibit flicker noise. A closely related issue is the existence of a low-frequency cutoff for the $1/f$ spectrum. Such a cutoff always exists whenever time scales are related to spatial scales, because any physical system is of finite spatial extent. Thus, the power spectra describing self-organized phenomena eventually deviate from the $1/f^\gamma$ law at low frequencies. On the other hand, quantum indeterminacy sets no low-frequency cutoff, and, as was demonstrated in Sec. III C, no such cutoff is needed to ensure finiteness of the voltage variance as long as $\gamma < 2$.

[1] J. B. Johnson, Phys. Rev. **26**, 71 (1925).

[2] M. Buckingham, *Noise in Electronic Devices and Systems* (Ellis Horwood, Chichester, 1983).

[3] D. A. Bell, J. Phys. C: Solid State Phys. **13**, 4425 (1980).

[4] A. K. Raychaudhuri, Curr. Opin. Solid State Mater. Sci. **6**, 67 (2002).

[5] B. V. Rollin and I. M. Templeton, Proc. Phys. Soc. B **66**, 259 (1953).

[6] M. F. Caloyannides, J. Appl. Phys. **45**, 307 (1974).

[7] J. H. Scofield, J. V. Mantese, and W. W. Webb, Phys. Rev. B **32**, 736 (1985).

[8] T. G. M. Kleinpenning and A. H. de Kuijper, J. Appl. Phys. **63**, 43 (1988).

[9] R. B. Ugryumov, A. V. Shaposhnik, and V. S. Voishchev, Tech. Phys. **49**, 941 (2004).

[10] B. Chenaud, A. Segovia-Mera, A. Delgard, N. Feltin, A. Hoffmann, F. Pascal, W. Zawadzki, D. Mailly, and C. Chaubet, J. Appl. Phys. **119**, 024501 (2016).

[11] J. F. Stephany, J. Phys.: Condens. Matter **12**, 2469 (2000).

[12] A. Van Der Ziel, Physica **16**, 359 (1950).

[13] A. L. MacWhorter, in *Semiconductor Surface Physics*, edited by R. H. Kingston (University of Pennsylvania Press, Philadelphia, 1956).

[14] D. A. Bell, *Electrical Noise* (Van Nostrand, London, 1960).

[15] K. A. Kazakov, J. Phys. A: Math. Theor. **40**, 5277 (2007).

[16] K. A. Kazakov, Phys. B: Condens. Matter **403**, 2255 (2008).

[17] K. A. Kazakov, Phys. Lett. A **384**, 126812 (2020).

[18] N. Wiener, Acta Math. **55**, 117 (1930).

[19] A. Khintchine, Math. Ann. **109**, 604 (1934).

[20] I. Flinn, Nature (London) **219**, 1356 (1968).

[21] V. B. Berestetskii, E. M. Lifshitz, and L. P. Pitaevskii, *Quantum Electrodynamics*, 2nd ed. (Pergamon Press, New York, 1982), Chap. XII.

[22] J. Schwinger, J. Math. Phys. **2**, 407 (1961).

[23] L. V. Keldysh, Zh. Eksp. Teor. Fiz. **47**, 1515 (1964) [Sov. Phys. JETP **20**, 1018 (1965)].

[24] S. Weinberg, *The Quantum Theory of Fields. Vol. 1: Foundations* (Cambridge University Press, Cambridge, UK, 1995).

[25] G. D. Mahan, *Many-Particle Physics* (Kluwer Academic/ Plenum Publishers, New York, 2000).

[26] K. E. El-Kelany, P. Carbonnière, A. Erba, and M. Rérat, J. Phys. Chem. C **119**, 8966 (2015).

[27] X. Wang, H. Tian, W. Xie, Y. Shu, W.-T. Mi, M. A. Mohammad, Q.-Y. Xie, Y. Yang, J.-B. Xu, and T.-L. Ren, NPG Asia Mater. **7**, e154 (2015).

[28] G. Mahan, in *Polarons in Ionic Crystals and Polar Semiconductors*, edited by J. T. Devreese (North-Holland, Amsterdam, 1972), p. 553.

[29] E. M. Lifshitz and L. P. Pitaevskii, *Physical Kinetics* (Pergamon Press, New York, 1981), Chap. X.

[30] N. P. Landsman and Ch. G. van Weert, Phys. Rep. **145**, 141 (1987).

[31] J. J. Brophy, J. Appl. Phys. **41**, 2913 (1970).

[32] M. S. Keshner, Proc. IEEE **70**, 212 (1982).

[33] As deduced from the original data provided by the authors of Ref. [10] (C. Chaubet, private communication).

[34] R. J. Hawkins, Ph.D. thesis, University of Southampton, Southampton, UK, 1970 (unpublished).

[35] R. J. Hawkins and G. G. Bloodworth, Thin Solid Films **8**, 193 (1971).

[36] T. G. M. Kleinpenning, J. Appl. Phys. **48**, 2946 (1977).

[37] J. A. Testa, Y. Song, X. D. Chen, J. Golben, S.-I. Lee, B. R. Patton, and J. R. Gaines, Phys. Rev. B **38**, 2922 (1988).

[38] K. A. Kazakov, Phys. Lett. A **373**, 4393 (2009).

[39] F. N. Hooge, Phys. Lett. A **29**, 139 (1969).

[40] Y. Song, A. Misra, P. P. Crooker, and J. R. Gaines, Phys. Rev. Lett. **66**, 825 (1991).

[41] W. J. Padilla, Y. S. Lee, M. Dumm, G. Blumberg, S. Ono, K. Segawa, S. Komiya, Y. Ando, and D. N. Basov, Phys. Rev. B **72**, 060511(R) (2005).

[42] H. Minami and H. Uwe, Physica C **282-287**, 1193 (1997).

[43] L. Liu, K. Zhang, H. M. Jaeger, D. B. Buchholz, and R. P. H. Chang, Phys. Rev. B **49**, 3679 (1994).

[44] H. Nyquist, Phys. Rev. **32**, 110 (1928).

[45] P. H. Handel, Phys. Rev. A **22**, 745 (1980).

[46] P. H. Handel, Phys. Rev. Lett. **34**, 1492 (1975).

[47] T. S. Sherif and P. H. Handel, Phys. Rev. A **26**, 596 (1982).

[48] A. van der Ziel and P. H. Handel, Physica B+C **132**, 367 (1985).

[49] P. H. Handel, in *Proceedings of the Eighth International Conference on Noise in Physical Systems and Fourth International Conference on 1/f Noise (Rome, 1985)*, edited by A. D'Amico and P. Mazzetti (North-Holland, Amsterdam, 1986), p. 465.

[50] P. H. Handel, Phys. Rev. A **38**, 3082 (1988).

[51] P. H. Handel, Phys. Status Solidi B **194**, 393 (1996).

[52] P. H. Handel, in *Proceedings of the 22nd International Conference on Noise and Fluctuations (ICNF), June 2013, Montpellier, France* (IEEE, Piscataway, NJ, 2013), p. 169.

[53] P. Bak, Ch. Tang, and K. Wiesenfeld, Phys. Rev. Lett. **59**, 381 (1987).

[54] P. Bak, Ch. Tang, and K. Wiesenfeld, Phys. Rev. A **38**, 364 (1988).